Sensors and Actuators, 1 (1981) 289 - 303

CHARACTERIZATION OF INTERFACES

G A BOOTSMA

Twente University of Technology, Department of Applied Physics, 7500 AE Enschede (The Netherlands)

1. Characteristics of solid surfaces

On the atomic scale the interfacial region of a solid is characterized by

(a) chemical composition types and concentrations of atoms,

(b) geometrical structure mutual arrangement of the atoms, long-range ordering, topography and defect structure,

(c) electronic properties surface potential, interface states

As a result of the tendency of minimalization of the Gibbs free energy, the geometric and electronic structures of the surface region of a crystal are often different from the bulk structure This has not only been established for substances with strong, covalent bonds (superstructures and surface states of semiconductors such as Si and Ge [1]), but also for metal surfaces (contraction between first and next atomic layers, especially on the less close-packed faces [2]) The transition region from the outer surface plane to the homogeneous bulk is called *selvedge* (Fig 1) Foreign atoms may become adsorbed on the surface or absorbed in the selvedge and bulk This often gives rise to the formation of ordered superstructures

The structure and electronic properties of single crystal surfaces are dependent on the crystallographic orientation of the surface plane This so-called *plane-specificity* is illustrated in Figs 2 and 3 by idealized models of the three low-index planes of the face-centered cubic (*e g* , Cu) and diamond (*e g* , Si) structures

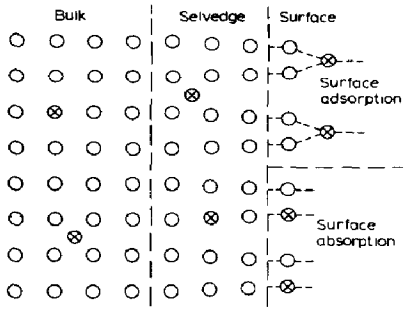

Fig 1 Schematic view of a planar cut into a crystalline solid showing surface, selvedge and bulk lattice atoms, open circles, foreign atoms, cross circles (from ref 3)

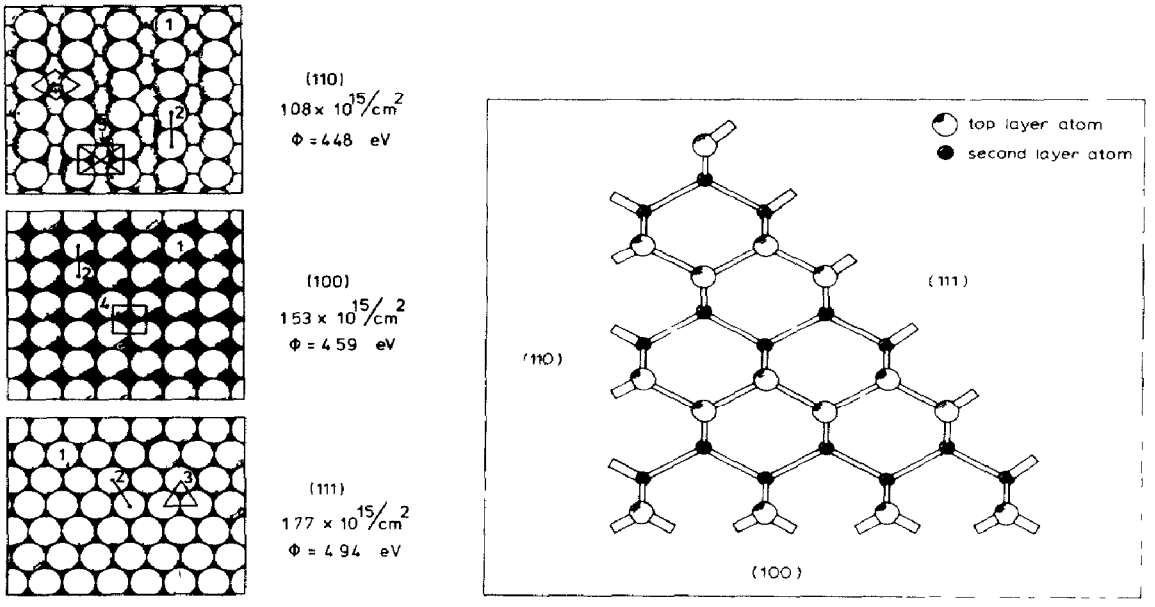

Fig 2 Ball models of copper single crystal surfaces The balls represent atoms and the ensembles of interconnected atoms represent sites of the type B_n with n as indicated Also given are the number of surface atoms per cm^2 and the photo-electric work function ϕ (from ref 4)

Fig 3 Idealized model of the silicon crystal with the three low-index planes The crystal is viewed along a [110] direction (from ref 5)

For Cu (lattice parameter a = 3 61 Å) the bulk density, N_b = 0 85 × 10^{23} atoms/cm^3, and the densities of the copper atoms in the different surface planes are as indicated in Fig 2 Of the 12 nearest neighbour atoms around an atom inside the bulk, 9, 8, and 7 are left around atoms in the (111), (100) and (110) plane, respectively The ideal low-index planes reveal both identical (B_1, B_2) and different, more specific (B_3, B_4, B_5) types of adsorption sites (see Fig 2) The work function appears to be larger for more densely packed surfaces

For Si (a = 5 42 Å, N_b = 0 50 × 10^{23} cm^{-3}) the density of the atoms in the (111), (100) and (110) plane is 0 78, 0 68 and 0 96 × 10^{15} cm^{-2}, respectively In obtaining these surfaces, of the 4 bonds to neighbouring atoms in the bulk, 1, 2, and 1 have to be broken, respectively, resulting in different types of adsorption sites (see Fig 3)

In reality, surfaces will not be as ideal as suggested by the models of Figs 2 and 3, but will exhibit a number of defects A schematic picture of a real surface is given in Fig 4, the so-called terrace–ledge–kink (TLK) model, developed by Kossel [6] and Stranski [7] Atomically flat terraces, with vacancies and ad-atoms, are separated by monatomic steps (or ledges) which themselves may exhibit kinks

The presence of a liquid medium in solid/liquid systems, in contrast to solid/gas systems, has a number of consequences [8]

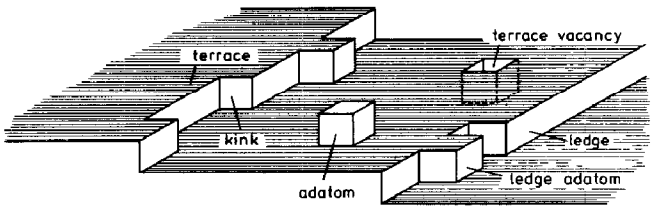

Fig 4 The terrace–ledge–kink model of a crystalline surface (from ref 4)

(a) Any charge on the solid surface causes a countercharge in the liquid (the electrical double layer) This can give rise to very steep potential gradients in concentrated electrolyte solutions ($\sim 10^9$ V m^{-1})

(b) In studying solid/gas interfaces, in order to prevent unwanted contamination of the surface, it is necessary to work in ultra high vacuum (UHV) conditions (background pressure $< 1\ 33 \times 10^{-7}$ Pa = 10^{-9} Torr) In solid/liquid studies (*e g*, interfacial electrochemistry) there is a need for ultra pure liquid solutions, to be achieved, for example, by pre-electrolysis or circulation over activated charcoal For the final cleaning of surfaces in a UHV system, methods such as ion sputtering, heating, cleaving, and gas etching are used Electrochemists often remove contaminants by desorption at a suitable potential or by destruction by anodic oxidation

(c) An important parameter in solid/gas studies is the gas pressure The equivalent parameter in solid/liquid systems is the concentration of an active species Moreover, electrochemists have an extra parameter the electrode potential In solid/gas studies, usually a much wider range of temperatures can be realized

2 Methods of characterization

Surface scientists have quite an arsenal of techniques at their disposal for investigating the chemical composition, geometrical structure, and electronic properties of solid surfaces Many combinations of incident, primary and detected, secondary particles (photons, $h\nu$, electrons, e, ions, I, and also neutrals) have been discovered and successfully developed into a technique A summary, with a few of the most frequently applied methods, is given in Table 1, for reviews see, *e g* , refs 9 - 12 A review of the present status and use of surface-characterization techniques in the U S A has recently been made by Powell [13] Very recently, Holloway and McGuire have presented a discussion of the application of AES, XPS, ISS and SIMS in the characterization of electronic devices and materials [14, with 440 refs]

A comparison of the various probes (Table 2) indicates that protons are less atom-specific (polarizability $\tilde{\alpha}$ *vs* electron energy scheme E_i^{el} or mass m) and less surface sensitive (larger information depth) than electrons and ions Moreover, the limit of detection of optical techniques is usually larger than in electron or ion spectroscopy However, by contrast with surface techniques employing electrons or ions, the influence of photons on the

TABLE 1

Summary of measurement techniques for surface characterization

Primary / Secondary	e	$h\nu$	I
e	LEED SEM (R)HEED TEM		
e'*	AES EELS	PES $\begin{matrix}\text{UPS}\\ \text{XPS}\end{matrix}$	
$h\nu$		IR spectroscopy reflectrometry ellipsometry	
$h\nu'$*		EXAFS RAMAN spectrosc	
I			ISS RBS
I'**	ESD		SIMS

AES	Auger electron spectroscopy
EELS	Electron energy-loss spectroscopy
ESD	Electron-stimulated desorption
EXAFS	Extended X-ray absorption fine structure
ISS	Ion scattering spectroscopy
LEED	Low-energy electron diffraction
PES	Photo-electron spectroscopy
RBS	Rutherford backscattering spectroscopy
(R)HEED	(Reflection) high energy electron diffraction
SEM	Scanning electron microscopy
SIMS	Secondary ion mass spectroscopy
TEM	Transmission electron microscopy
UPS	Ultraviolet photoemission spectroscopy
XPS	X ray photoemission spectroscopy
*e', $h\nu'$	energy different from primary energy
**I'	mass different from primary mass

studied samples and processes is generally negligible and *in situ* measurements at high gas pressures or with liquids are possible

Techniques involving the passage of electrons or ions through the system require high vacuum and are not directly applicable in solid/liquid studies, and they can only be used to investigate the state of the solid surface before and/or after an experiment The solid sample has to be removed from the liquid, which may lead to chemical changes, *e g* , because of the loss of control of the electrical potential or because of contamination during the transfer to the UHV chamber Attempts to reduce this risk involve attaching the electrochemical cell directly to the UHV chamber [15, 16] or the use of specially designed thin layer cells which are kept inside UHV chambers [17, 18]

TABLE 2

Properties and limitations of surface probes

	e (AES, PES)	I (ISS, SIMS)	$h\nu$ (reflect , ellips)
Energy (eV)	10 - 1000	10^2 - 10^6	1 10
Parameter	E_1^{el}	m	$\tilde{\alpha}$
Information depth (ML)	2 - 10	1	10 - 10^4
Detection limit (ML)	10^{-2} - 10^{-4}	10^{-3} - 10^{-6}	10^{-1} - 10^{-2}
Limitation	UHV, ESD ESA	UHV, sputtering damage, implantation	

3. Optical techniques

3 1 Introduction

Table 3 surveys the various regions of wavelength, λ, and energy, $E = h\nu = hc/\lambda$, of the electromagnetic spectrum, where ν is the frequency, c the speed of the waves in vacuum (c = 3 0 × 10^8 m s^{-1}) and h the Planck constant (h = 6 63 × 10^{-34} J s) Also indicated are the different types of probed atomic or molecular transitions

In general, two groups of optical methods may be distinguished, depending on the energy relation between incident and detected beams In the first group the wavelength remains the same, and changes in intensity or state of polarization of the light beam at a given (eventually varying) λ are measured In the second group the excitation and scattering processes result in a change in λ Examples of the first group are the various types of absorption spectroscopy and ellipsometry, to the second group belong Raman spectroscopy and photoacoustic spectroscopy

Recently, Raman spectroscopy has aroused attention as a molecularly specific probe in surface chemistry because of the enormous enhancement (by as much as 10^6) of the Raman cross section of adsorbates on metal electrodes in an electrochemical environment compared with the isolated molecules in solution [19, 20] There appears to be fairly general agreement that the roughness of the surface plays an important role in the enhancement, but there is no agreement yet as to the scale of this roughness nor to the basic mechanism [21]

Photoacoustic spectroscopy involves the determination of the optical absorption spectrum of interfacial layers by illuminating the surface by light modulated at audio frequencies and then detecting the thermally generated sound waves in the ambient phase as a function of optical wavelength [22, 23] The advantage over reflectrometric methods is that the samples can have all kinds of shapes and dimensions dispersed, powdered specimens can

TABLE 3

Electromagnetic waves

	X-rays	UV	visible	IR	microwaves	
λ (Å)	0 1	100	4000	7000	10^7	10^9
E (eV)	$1\,2 \times 10^5$	120	3 1	1 8	$1\,2 \times 10^{-3}$	$1\,2 \times 10^{-5}$

electronic transitions — vibrations — rotations

be analyzed as well as macroscopic crystals with well-defined surfaces For spectra from thin films on metals, sensitivities better than 10^{-2} monolayer have been reported [24]

Figure 5 shows the principles of the optical techniques in which the wavelengths of the primary and secondary beams are the same Intensity changes are measured as a function of λ in transmission spectroscopy, internal reflection spectroscopy, and external reflection spectroscopy, mostly in the region of the spectrum where vibrational transitions take place Transmission spectra have been obtained for species adsorbed onto dispersed substrates, usually pressed into a thin disk [25 - 27] Multiple internal reflection methods demand special sample designs and can only be applied in λ regions where the bulk substrate is transparent [28] External reflection spectroscopy has a much broader applicability, for example, electroreflectance measurements at solid/electrolyte interfaces have been carried out to determine change with potential, and differential reflectance spectroscopy and related modulation techniques have been applied to the study of adsorption processes and film formation [29 - 31]

Ellipsometry involves the measurement of the change in the state of polarization that occurs when a monochromatic beam of polarized light is reflected from (or transmitted through) an interface [32 - 36] The advantage of this technique is its high sensitivity (down to ~0 01 of a monolayer of adsorbed atoms can be detected) and the fact that two (eventually three) experimental quantities are determined at a given λ

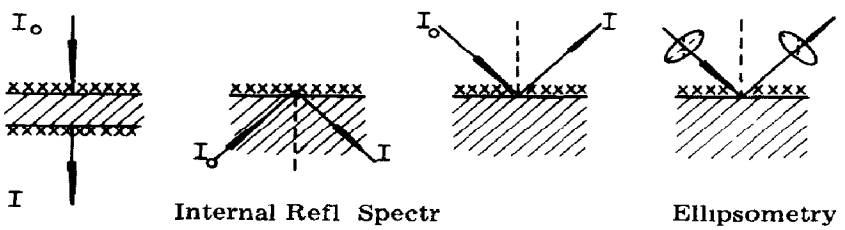

Fig 5 Principles of optical methods measuring changes in intensity or state of polarization

Detailed information on the techniques and their applications is found in the indicated review papers In the next section the principles of ellipsometry and differential reflectrometry will be briefly described

3 2 Ellipsometry and differential reflectrometry

The state of polarization of a polarized light beam is characterized by the phase and amplitude relations of the two components into which the total electrical-field vector, $\vec{E}$, of the light wave can be resolved These components are chosen parallel with (E_p) and perpendicular to (E_s) the plane of incidence

$$E_p = A_p \exp i(\omega t + \delta_p), \tag{1a}$$

$$E_s = A_s \exp i(\omega t + \delta_s), \tag{1b}$$

where ω is the angular frequency ($2\pi\nu$) In general, upon reflection a change will occur, both in the phases, δ, and in the amplitudes, A, of the two components These changes are described by the two parameters Δ and ψ, defined as

$$\Delta = (\delta_p{}^r - \delta_s{}^r) - (\delta_p{}^i - \delta_s{}^i), \tag{2}$$

$$\tan \psi = \frac{A_p{}^r}{A_s{}^r} \Big/ \frac{A_p{}^i}{A_s{}^i}, \tag{3}$$

where the superscripts r and i correspond to the reflected and incident beams The parameters Δ and ψ are measured with the ellipsometer The total effect upon reflection is summarized in the equation

$$\frac{r_p}{r_s} = \frac{E_p{}^r}{E_s{}^r} \Big/ \frac{E_p{}^i}{E_s{}^i} = \tan \psi \exp(i\Delta) \tag{4}$$

Here r_p and r_s are the amplitude reflection coefficients, which can be expressed as functions of λ, the angle of incidence, ϕ_0, and the optical parameters of the reflecting system (see Fig 6) If one uses the representation $\tilde{n} = n - ik$ for the complex index of refraction, and Snell's law

$$n_0 \sin \phi_0 = \tilde{n}_1 \sin \tilde{\phi}_1 \tag{5}$$

to define the complex angle of refraction at a single optical boundary (Fig 6(a)), r_p and r_s take the form of the Fresnel coefficients

Fig 6 Schematic representation of the reflection of polarized light (a) Clean surface, (b) surface covered with single layer

$$r_p = \frac{\tilde{n}_1 \cos\phi_0 - n_0 \cos\tilde{\phi}_1}{\tilde{n}_1 \cos\phi_0 + n_0 \cos\tilde{\phi}_1} , \tag{6a}$$

$$r_s = \frac{n_0 \cos\phi_0 - \tilde{n}_1 \cos\tilde{\phi}_1}{n_0 \cos\phi_0 + \tilde{n}_1 \cos\tilde{\phi}_1} \tag{6b}$$

In this case the measured Δ and ψ values yield the optical constants of the reflecting material the refractive index n_1 and the extinction coefficient k_1

For a substrate covered with a layer (Fig 6(b)) r_p and r_s take the form

$$r_p = \frac{r_{Ip} + r_{IIp} \exp(-ix_1)}{1 + r_{Ip} r_{IIp} \exp(-ix_1)} , \tag{7a}$$

$$r_s = \frac{r_{Is} + r_{IIs} \exp(-ix_1)}{1 + r_{Is} r_{IIs} \exp(-ix_1)} \tag{7b}$$

Here r_I and r_{II} are the Fresnel coefficients at interface 0–1 and 1–2, respectively, and x_1 denotes the phase difference due to one internal reflection within the layer

$$x_1 = \frac{4\pi}{\lambda} \tilde{n}_1 d_1 \cos\tilde{\phi}_1 \tag{8}$$

So for this system we have, by combining eqns (4) - (8)

$$\tan\psi \exp(i\Delta) = f(\lambda, \phi_0, n_0, n_1, k_1, d_1, n_2, k_2) \tag{9}$$

The parameters λ, ϕ_0, and n_0 are usually known and, in many cases also, the substrate optical constants n_2 and k_2 The changes in Δ and ψ upon formation of a layer are then given by

$$\delta\Delta = \bar{\Delta} - \Delta , \tag{9a}$$

$$\delta\psi = \bar{\psi} - \psi , \tag{9b}$$

and

$$\delta\Delta, \delta\psi = f(\text{known parameters}, n_1, k_1, d_1) \tag{10}$$

Here $\bar{\Delta}$ and $\bar{\psi}$ refer to the clean substrate, and Δ and ψ to the substrate covered with a layer The problem of deriving three unknowns from two measured parameters has been solved by variation of ϕ_0, n_0 or d_1 (all under the assumption that the outer optical parameters remain constant), or by making a suitable choice of the value of one of the unknowns based on other experiments In some cases the measurement of a third experimental quantity, the change in intensity, can yield a solution

The change in intensity upon reflection, or the reflectivity, R, is given by

$$R_{p,s} = r_{p,s} r^*_{p,s} = |r_{p,s}|^2 , \tag{11}$$

where r^* is the complex conjugate of r At normal incidence ($\phi_0 = 0°$), one obtains for reflection at a clean substrate, from eqns (6) and (11),

TABLE 4

Sensitivity of ellipsometry ($\phi_0 = 70°$) and differential reflectometry ($\phi_0 = 0°$), $n_0 = 1$, $\lambda = 5500$ Å, $n_1 = 1.5$

	Si	Fe	Ni
n_2	4.05	3.12	1.79
k_2	0.028	3.87	1.83
ζ(deg/Å)	0.32	0.18	0.10
η(deg/Å)	0.001	0.021	0.030
$\frac{\Delta R}{R}$(Å^{-1})	-5.5×10^{-6}	-2.2×10^{-4}	-8.5×10^{-4}

$$R_p = R_s = \left|\frac{\tilde{n}_1 - n_0}{\tilde{n}_1 + n_0}\right|^2 \tag{12}$$

When the layer on the clean substrate is very thin ($d_1 \ll \lambda$) eqn (10) may be approximated as (see ref. 37)

$$\delta\Delta = \zeta(\lambda, \phi_0, n_0, n_1, k_1, n_2, k_2)\, d_1 \ , \tag{13a}$$

$$\delta\psi = -\eta(\lambda, \phi_0, n_0, n_1, k_1, n_2, k_2)\, d_1 \tag{13b}$$

Although computer calculations with the exact equations are easily performed (*e.g.*, by using the program of McCrackin [38]) the estimated values of ζ and η give an impression of the sensitivity of the method. In Table 4 some examples are presented. Since $\delta\Delta$ and $\delta\psi$ can be measured with an accuracy of ~0.01°, thicknesses of the order of 0.1 Å can be determined.

In *differential reflectometry* the measured quantity is the relative change in reflectivity

$$\frac{\Delta R}{R} = \frac{R(d_1) - R(0)}{R(0)} \ , \tag{14}$$

where $R(d_1)$ is the reflectivity of the system, ambient/layer/substrate (Fig. 6(b)) and $R(0)$ that of the system ambient/substrate (Fig. 6(a)). $R(0)$ is calculated from eqns. (6) and (11), $R(d_1)$ from eqns. (7) and (11). When $d_1 \ll \lambda$, one gets, in first order approximation [39, 30], at normal incidence on a substrate under vacuum

$$\frac{\Delta R}{R} = \frac{8\pi d_1}{\lambda} \operatorname{Im}\left(\frac{\tilde{\epsilon}_1 - \tilde{\epsilon}_2}{1 - \tilde{\epsilon}_2}\right) \tag{15}$$

Here $\tilde{\epsilon}$ is the complex dielectric constant, $\tilde{\epsilon} = \epsilon' - i\epsilon''$, which is related to $\tilde{n}$ by

$$\tilde{\epsilon} = \tilde{n}^2 \text{ and thus } \epsilon' = n^2 - k^2, \ \epsilon'' = 2nk \tag{16}$$

The calculated examples in Table 4 illustrate that here also thicknesses of the order of 0.1 Å may be determined, since the differential reflectivity can

be measured with an accuracy of $\sim 10^{-4}$ [5] In both methods the sensitivity depends on the relative values of $\tilde{n}_1$ and n_0, $\tilde{n}_2$, and therefore also on the wavelength

4 Applications

4 1 Adsorption from the gas phase

The sensitivity of ellipsometry and differential reflectometry enables one to detect layers with an effective thickness of the order of 1 - 10% of the monolayer In the macroscopic description, an adsorbed (sub)monolayer is idealized as homogeneous with thickness d_1 and index of refraction n_1, as in Fig 6(a) It has been shown that for *physisorption*, where the interaction between adsorbate and substrate is weak, *e g* , krypton on silicon and germanium [37, 40] and zenon on graphite [41], the ellipsometric results could be interpreted with a simple extrapolated macroscopic theory in which the relation between n_1 and the microscopic parameters is given by the Lorentz–Lorenz equation

$$\frac{n_1^2 - 1}{n_1^2 + 2} = \frac{\alpha\theta}{3\sigma_m d_m} \tag{17}$$

Here α is the polarizability, σ the cross-sectional area, θ the degree of coverage ($\theta = \sigma_m/\sigma$, with σ_m cross-section at $\theta = 1$) and d_m the diameter of the adsorbed atoms or molecules In good approximation, one gets for eqns (13a, b)

$$\delta\Delta = C(\lambda, \phi_0, n_0, n_2, k_2)\frac{\alpha\theta}{\sigma_m} \quad , \tag{18a}$$

$$\delta\psi \approx 0 \tag{18b}$$

For *chemisorption*, where changes in the optical properties of the substrate can be induced, the interpretation is more complicated The ellipsometric results obtained for chemisorption of various gases, *e g* , oxygen, on clean semiconductor surfaces, *e g* , Si and Ge, could be interpreted with a model in which a transition layer at the clean surface, with optical properties different from the bulk ($\tilde{n}_2^{ss}$, associated with surface states), is effectively removed (Fig 7(a)) [40, 43] Measurements at various wavelengths yielded a joint density-of-states curve for optical transitions from filled dangling-bond surface states to empty bulk-conduction or surface-states bands [43] It can be shown [5] that the joint-density-of-states function $J(\nu)$ for these transitions

$$J(\nu) \propto (h\nu)^2 \mathrm{Im}(\tilde{\epsilon}_{ss} - \tilde{\epsilon}_2) \tag{19}$$

Comparison with eqn (15) indicates that differential reflectometric measurements of the adsorption of oxygen on clean silicon surfaces directly yield $\mathrm{Im}(\tilde{\epsilon}_{ss} - \tilde{\epsilon}_2)$ or $J(\nu)$, provided that the optical effects of the oxygen layer

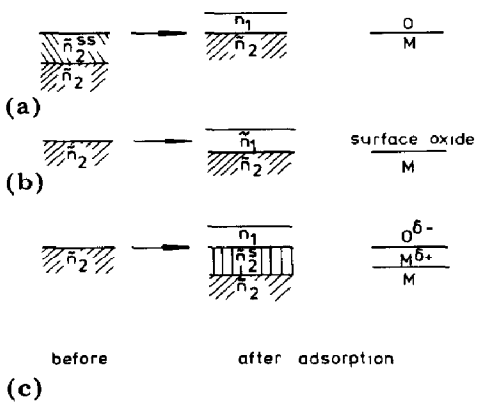

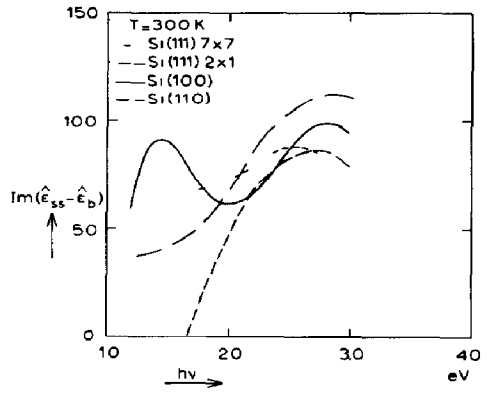

Fig 7 Optical models of chemisorption of oxygen

Fig 8 Surface-state transitions on the low-index planes of silicon at 300 K determined by differential reflectometry (from ref 5)

(with refractive index n_1 in Fig 7(a)) can be neglected (*cf* Table 4) and that a value is chosen for the thickness of the surface-states layer d_{ss} However, as can be seen from eqn (15), the choice of d_{ss} does not influence the shape of the $\mathrm{Im}(\tilde{\epsilon}_{ss} - \tilde{\epsilon}_2)$ *versus* $h\nu$ curves Results of the differential reflectometry study of Wierenga [5, 44] on various silicon planes are summarized in Fig 8 In the energy region of 1 - 3 eV for all surfaces, a mean peak in $J(\nu)$ is found at 3 0 eV and for some surfaces also a peak at lower frequencies

From eqns (15) and (19) it follows that the change in reflectivity upon oxygen adsorption is proportional to the number of surface states which have disappeared By measuring $\Delta R/R$, at a given photon energy, as a function of oxygen exposure, the kinetics of the adsorption of oxygen on those surface atoms which contribute to the surface-state transitions at that energy, could be determined for the various silicon planes [5]

With the combination ellipsometry–AES–LEED, linear relationships have been observed between $\delta\Delta$ at λ = 6328 Å and the oxygen coverage, θ, in the chemisorption stage ($\theta < 0$ 5 oxygen atoms/metal surface atom) on Ag(110) [46], Cu(111) [47], Cu(110) [48] and Cu(100) [49] This has been applied to determine the kinetics of the adsorption of O_2 and N_2O, and of the removal of adsorbed oxygen by CO For Ni(100) the Δ changes in the first chemisorption stage were too small to derive a reliable coverage dependence [50] After the first stage, a further, much slower uptake (incorporation) of oxygen takes place on Cu [49, 51] and on Ni [50], accompanied by a reconstruction of the surface The ellipsometric effects per incorporated atom are smaller for Cu and larger for Ni as compared with the effects per chemisorbed oxygen atom To explain the observed values of $\delta\Delta$ and $\delta\psi$, changes in the substrate have to be taken into account The model used for chemisorption on semiconductor surfaces (Fig 7(a)) cannot explain the data, more appropriate models appeared to be those depicted in Fig 7(b), (c) [52] In fact model (c) (adsorption of $O^{\delta-}$ ions on a positively charged metal surface layer) is a detailed version of model (b) (formation of a surface oxide with effective index of refraction $\tilde{n}_1$)

The gas phase studies showed that the chemisorptions of O_2 and N_2O on silver and copper single crystal surfaces are very plane-specific reactions and that the order of the reaction rates is (110) > (100) > (111) The oxidation of CO to CO_2 by pre-adsorbed oxygen appears to be non plane-specific

4 2 Solid/electrolyte interface

Compared with solid/gas interface studies, the *in situ* investigations of solid/electrolyte interfaces with ellipsometry and reflectometry usually show a lower sensitivity and are more difficult to interpret The lower sensitivity is caused by the fact that the refractive index, n_0, of the ambient liquid phase (for aqueous solutions in the visible region $n_0 \approx 1\ 33$) is much closer to the effective value of n_1 of most interfacial layers than is n_0 of vacuum or air ($n_0 = 1\ 0$) The interpretation of the optical results is often complicated by the simultaneous occurrence of several processes, *e g* , double layer formation in the solid and liquid phases, specific adsorption, changes in morphology of the interface due to dissolution and formation of interfacial layers, which all may affect the optical properties Moreover, the lack of other molecularly specific *in situ* probing techniques precludes investigations in combination with other methods, apart from the very sensitive but not specific electrochemical methods For reviews on the application of ellipsometry in electrochemistry, see, *e g* , refs 32, 53, 54 By way of illustration a few examples will briefly be mentioned here

The optical effect of electrical double layers at electrode/electrolyte interfaces has been estimated by Stedman for Hg/NaF solution [55] by using the Gouy–Chapman model and assuming that the excess charge of the species in the diffuse layer is concentrated in a single homogeneous layer with a thickness equal to twice the double-layer thickness The effective refractive index of this layer was calculated with the Lorentz–Lorenz equation (*cf* eqn (17)) Albers [56] has carried out calculations for AgI/KNO_3 solution with a more detailed, multilayer model, including a Stern layer with specifically adsorbed hydrated ions and a diffuse layer composed of several thin films with gradually varying index of refraction Both authors came to the conclusion that even at high surface charges ($\sim 20\ \mu C/cm^2$) the ellipsometric effects due to the formation of the double layer are small ($\delta\Delta \approx 0\ 1 - 0\ 2°$)

Very recently, Droog has reported on a study of the anodic oxidation of silver and copper electrodes in alkaline solutions by using electrochemical techniques (a o potential sweep voltammetry) in combination with ellipsometry [8] The formation of bulk silver oxide on polycrystalline silver [57] and on Ag(111) and (110) surfaces [58] is preceded by dissolution of silver species, and deposition of monolayer amounts of a surface oxide, at potentials that are more cathodic than the reversible potential for the deposition of bulk Ag_2O Ellipsometry was used to discriminate between surface oxide formation and dissolution of silver species With increasing scan rate, $\delta\Delta$ decreases much more slowly than the charges under the anodic (Q_a) and cathodic (Q_c) curves in the earliest stages of the oxidation (Fig 9) This implies that an increasing fraction of the total current must be ascribed to

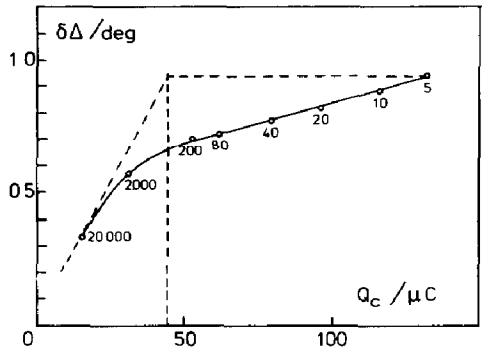

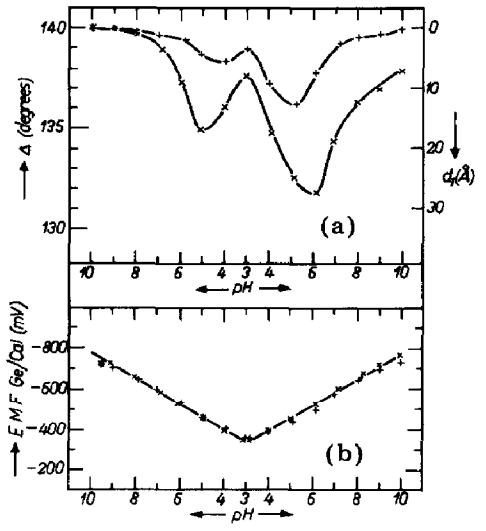

Fig 9 $\delta\Delta$ *vs* Q_c for voltammograms taken with different sweep rates for polycrystalline Ag in 1M NaOH, 22 °C Numbers in the Figure indicate sweep rates in V s^{-1} Double layer contributions to $\delta\Delta$ and Q_c are taken to be 0 2° and 8 μC, respectively (from ref 57)

Fig 10 Results of the ellipsometric (a) and cell potential (EMF) (b) measurements *vs* pH of a germanium electrode in a solution containing 10^{-2}M H_2O_2 and 0 1M KCl (+) or 1M KCl (x) The points were measured at time intervals of 15 min The film thickness d_1 was calculated using eqn (13a) with ζ = 0 3 deg /Å (from ref 60)

chemisorption of oxygen As in the gas phase, the Ag(110) face appeared to be much more reactive to oxygen than the (111) face A same plane-specific electrosorption behaviour was observed for oxygen on Cu single crystal surfaces [8] By contrast with Ag, for Cu no evidence was found for dissolution of copper species, $\delta\Delta$ and Q_a showed an identical dependence on the sweep rate [59]

The last example concerns an ellipsometric investigation of the film growth at the germanium/electrolyte interface [60] When placed in solutions containing hydrogen peroxide and potassium chloride, germanium electrodes show a perfect Nernst behaviour over a large range of pH values Results of ellipsometric and cell potential (Ge *vs* calomel electrode) measurements indicated that in the presence of H_2O_2 and KCl a very well-defined film formation takes place (Fig 10) The Δ-values at the starting point at pH = 10 correspond with the value calculated for the clean surface At lower pH a film is formed, probably an oxidation product of germanium, which is readily dissolved at high and low pH and is insoluble in the intermediate pH region Without H_2O_2 and/or KCl, however, no significant changes in Δ as a function of pH were observed, and the otherwise reproducible starting point at pH = 10 is not obtained The perfect Nernst dependence is evidently connected with an interfacial region in which the thermodynamic potentials of the components taking part in the redox reaction are clearly defined and related to the Fermi potential in the bulk of the germanium

References

1 F Meyer and M J Sparnaay, in C G Scott and C E Reed (eds), *Surface Physics of Phosphors and Semiconductors*, Academic Press, London, 1975, p 391
2 G A Somorjai and M A van Hove, *Struct Bonding (Berlin), 38* (1979) 1
3 H D Hagstrum, *Science, 178* (1972) 275
4 F H P M Habraken, Sorption and Reactivity of Oxygen on Copper Single Crystal Surfaces, *Thesis, Univ Utrecht, 1980*
5 P E Wierenga, Reflectometric Study of Surface States and Oxygen Adsorption on Clean Silicon Surfaces, *Thesis, Tech Univ Twente, Enschede, 1980*
6 W Kossel, *Nachr Ges Wiss Gottingen, Math Phys Kl , 135* (1927)
7 I N Stranski, *Z Phys Chem , 136* (1928) 259
8 J M M Droog, Anodic Oxidation of Silver and Copper in Alkaline Solutions, *Thesis, Univ Utrecht, 1980*
9 J M Blakely, *Introduction to the Properties of Crystal Surfaces*, Pergamon, Oxford, 1973
10 J Oudar, *Physics and Chemistry of Surfaces*, Blackie, Glasgow, 1975
11 M Prutton, *Surface Physics*, Clarendon, Oxford, 1975
12 A W Czanderna (ed), *Methods of Surface Analysis*, Elsevier, Amsterdam, 1975
13 C J Powell, *Appl Surf Sci , 1* (1978) 143
14 P H Holloway and G E McGuire, *Appl Surf Sci , 4* (1980) 410
15 R W Revie, J O'M Bockris and R G Baker, *Surf Sci , 52* (1975) 664
16 R O Ansell, T Dickinson, A F Povey and P M A Sherwood, *J Electroanal Chem , 98* (1979) 69
17 R M Ishikawa and A T Hubbard, *J Electroanal Chem , 69* (1976) 317
18 W E O'Grady, M Y C Woo, P L Hagans and E Yeager, *J Vac Sci Technol , 14* (1977) 365
19 M Fleischmann, P J Hendra and A J McQuillan, *Chem Phys Lett , 26* (1974) 163
20 R P van Duyne, in Optics at the Solid–Liquid Interface, Coll Int CNRS, *J Phys (Paris), C5* (1977) 239
21 A Otto, *Surf Sci , 92* (1980) 145, J Billmann, G Kovacs and A Otto, *Surf Sci , 92* (1980) 153
22 A Rosencwaig, *Anal Chem , 47* (1975) 592 A
23 N C Fernelius, *Appl Surf Sci , 4* (1980) 401
24 S O Kanstad and P E Nordal, *Ned Tijdschr Vacuumtech , 18* (1980) 65
25 L H Little, *Infrared Spectra of Adsorbed Species*, Academic Press, London, 1966
26 M L Hair, *Infrared Spectroscopy in Surface Chemistry*, Marcel Dekker, New York, 1967
27 A V Kiselev, *IR Spectra of Surface Compounds*, Wiley - Interscience, New York, 1975
28 N J Harrick, *Internal Reflection Spectroscopy*, Wiley - Interscience, New York, 1967
29 J D E McIntyre, in *Advances in Electrochemistry and Electrochemical Engineering*, Vol 9, Wiley - Interscience, New York, 1973, p 61
30 J D E McIntyre, in B O Seraphin (ed), *Optical Properties of Solids — New Developments*, North Holland, Amsterdam, 1976, p 555
31 D M Kolb, in Optics at the solid–liquid interface, Coll Int CNRS, *J Phys (Paris), C5* (1977) 167
32 W Paik, in J O'M Bockris (ed), *MTP International Review of Science, Electrochemistry*, Butterworths, London, 1973, p 239
33 R H Muller, in *Advances in Electrochemistry and Electrochemical Engineering*, Vol 9, Wiley - Interscience, New York, 1973, p 167
34 R M A Azzam and N M Bashara, *Ellipsometry and Polarized Light*, North-Holland, Amsterdam, 1977
35 W E J Neal, *Appl Surf Sci , 2* (1979) 445

36 Conf Proc
(a) E Passaglia R R Stromberg and J Kruger (eds), Ellipsometry in the Measurement of Surfaces and Thin Films, *Misc Publ 256*, Nat Bur Stand (US), Washington, DC, 1964
(b) N M Bashara, A B Buckman and A C Hall (eds), Recent developments in ellipsometry, *Surf Sci* , *16* (1969)
(c) N M Bashara and R M A Azzam (eds), Ellipsometry, *Surf Sci* , *56* (1976)
(d) D E Aspnes, R M A Azzam and R H Muller (eds), Ellipsometry, *Surf Sci* , *96* (1980)
37 G A Bootsma and F Meyer, *Surf Sci* , *14* (1969) 52
38 F L McCrackin, FORTRAN program for analysis of ellipsometer measurements, *Nat Bur Stand (US), Tech Note 479*, Washington, DC, 1969
39 J D E McIntyre and D E Aspnes, *Surf Sci* , *24* (1971) 417
40 F Meyer, E E de Kluizenaar and G A Bootsma, *Surf Sci* , *27* (1971) 88
41 G Quentel, J M Rickard and R Kern, *Surf Sci* , *50* (1975) 343
42 G Quentel and R Kern, *Surf Sci* , *55* (1976) 545
43 F Meyer, *Surf Sci*, *56* (1976) 37
44 P E Wierenga, A van Silfhout and M J Sparnaay, *Surf Sci* , *87* (1979) 43
45 P E Wierenga, M J Sparnaay and A van Silfhout, *Surf Sci* , *99* (1980) 59
46 H Albers, W J J van der Wal, O L J Gijzeman and G A Bootsma, *Surf Sci* , *77* (1978) 1
47 F H P M Habraken, E Ph Kieffer and G A Bootsma, *Surf Sci* , *83* (1979) 45
48 F H P M Habraken and G A Bootsma, *Surf Sci* , *87* (1979) 333
49 F H P M Habraken, C M A M Mesters and G A Bootsma, *Surf Sci* , *97* (1980) 264
50 P K de Bokx, F Labohm, O L J Gijzeman, G A Bootsma and J W Geus, *Appl Surf Sci* , *5* (1980) 321
51 F H P M Habraken, G A Bootsma, P Hofmann, S Hachicha and A M Bradshaw, *Surf Sci* , *88* (1979) 285
52 F H P M Habraken, O L J Gijzeman and G A Bootsma, *Surf Sci* , *96* (1980) 482
53 J Kruger, in *Advances in Electrochemistry and Electrochemical Engineering*, Vol 9, Wiley-Interscience, New York, 1973, p 227
54 Optics at the solid–liquid interface, Coll Int CNRS, *J Phys (Paris), C5* (1977)
55 M Stedman, *Symp Faraday Soc* , *4* (1970) 64, *Chem Phys Lett* , *2* (1968) 457
56 H Albers, unpublished
57 J M M Droog, P T Alderliesten and G A Bootsma, *J Electroanal Chem* , *99* (1979) 173
58 J M M Droog, *J Electroanal Chem* , to be published
59 J M M Droog, C A Alderliesten, P T Alderliesten and G A Bootsma, *J Electroanal Chem* , *111* (1980) 61
60 G A Bootsma and F Meyer, *Surf Sci* , *7* (1967) 250